Influence of the synthesis parameters on the efficiency of fluorescent ion-imprinted polymers for lead detection

William René, Véronique Lenoble, Katri Laatikainen, Bruno Viguier, Catherine Branger

Influence of the synthesis parameters on the efficiency of fluorescent ion-imprinted polymers for lead detection

William René, Katri Laatikainen, Bruno Viguier, Catherine Branger, Véronique Lenoble

Influence of the synthesis parameters on the efficiency of fluorescent ion-imprinted polymers for lead detection

William René[a,b], Véronique Lenoble[b*], Katri Laatikainen[c], Bruno Viguier[a], Catherine Branger[a*]

[a] Université de Toulon, MAPIEM, Toulon, France

[b] Université de Toulon, Aix Marseille Université, CNRS, IRD, MIO, Toulon, France

[c] Laboratory of Computational and Process Engineering, Lappeenranta-Lahti University of Technology LUT, P.O. Box 20, FI-53851 Lappeenranta, Finland

* Corresponding authors: lenoble@univ-tln.fr, branger@univ-tln.fr

ABSTRACT

New fluorescent ion-imprinted polymers (IIPs) specific for Pb(II) detection were synthesized by precipitation polymerization. The fluorescent activity of the IIPs was provided by a fluorescent functional monomer, ANQ-ST, based on the chelating 5-amino-8-hydroxyquinoline moiety coupled to anthracene and ~~to~~ a styrenic group. Various synthesis parameters were tested: metal/functional monomer ratio, polymerization solvent and crosslinker (ethyleneglycol dimethacrylate, EGDMA, or divinylbenzene, DVB). The characterization of the different IIPs was carried out by solid-state ^{13}C NMR spectroscopy, to analyse the structure of the polymers and to attest the integration of the ANQ-ST in the polymer matrix, and by scanning electron microscopy and nitrogen adsorption/desorption experiments, to study the morphology of the prepared materials. After characterization, the IIPs and their corresponding non-imprinted polymer (NIPs) were subjected to various fluorescence studies, in order to conclude on the influence of the synthesis parameters onto the polymer properties. The results demonstrated that the IIP synthesized with a metal/functional monomer ratio of 0.42 in DMSO/MeOH (1:1, v/v) and using EGDMA as a crosslinker was very sensitive to the presence of Pb(II) ions and almost not to ~~that of the~~ other tested ions (Ag(I), Na(I), Ca(II), Cd(II), Co(II), Cu(II) and Zn(II)), even ~~when they were~~ introduced in high excess. Calibration curves were performed in various matrices: ultra-pure water, buffered water at pH 7.0 and 8.1, seawater, tap water. They highlighted the low impact of the tested matrices onto the detection and allowed to determine a limit of detection of 2.4 µg/L and a linear range of 8.0-50 µg/L. Finally, the very good recovery obtained in natural samples emphasized the potential for the synthesized IIP to detect Pb(II) in natural waters.

Keywords: molecularly imprinted polymer, smart material, fluorescent sensor, lead, 5-amino-8-hydroxyquinoline

1. Introduction

Lead is a chemical element ~~which~~ that, like most metals, does not present any biochemically essential ~~function~~ role and causes the dysfunction of multiple organs within the human or animal body [1]. At worse, death results from a concentration of lead (Pb) in the human blood above 150 µg/dL [2]. Pb was used ~~during~~ for many centuries in pipes, pottery, arms industry and paints until the 19th and its usage is now declining [3]. Yet, there are still public health concerns, especially ~~concerning~~ related to mining activities [4], contaminated sediments resuspension [5], lead-based paints and drinking waters in low and middle-income developing countries [6,7] or some specific sources like syrups in Nigeria [8] or turmeric in Bangladesh [9]. ~~On~~ From an environmental point of view, a recent review demonstrated that the higher Pb load in urban areas also impacts the fauna and flora (pets and plants) and the water runoff herein [10]. Such urban runoff was identified as the major source of Pb in surface waters [11]. The Pb level in these waters is strictly regulated, for example in Europe [12] or the USA [13] to better take into account Pb toxicity on humans and ecosystems. Therefore, the monitoring of lead is necessary to assess the scientific advances, to improve governmental policies and to propose ~~a~~ supervision at local and national levels.

The design of sensors based on molecularly imprinted polymers (MIPs) was explored soon after the development of MIPs [14] and is continuously increasing (with over 350 papers per year in the last 3 years) [15]. The huge interest for MIPs in this field relies on their selective recognition ability that renders them excellent candidates as synthetic receptors for chemical sensors [16–18]. This intrinsic property is originating from their preparation mode: they are highly crosslinked polymers synthesized in the presence of a template (molecule, ion or protein) after a preliminary self-assembly step with at least one functional monomer. The removal of the template creates cavities inside the polymer network that can selectively rebind this target during the sensor use while associated with a mass, electrical or optical transducing mode. When metal ions are targeted, sensors prepared with ion-imprinted polymers (IIPs) are mainly based on electrochemical measurements because of the electro-activity of these ions [19–22]. However, optical-based sensors, and particularly fluorescent ones, are highly sensitive and adapted to miniaturization. Moreover, the analysis of a fluorescence signal can provide a lot of information through the analysis of excitation and emission spectra as well as fluorescence intensity, lifetime, and anisotropy [23]. As they do not have any fluorescent intrinsic property, the design of fluorescent sensors for metal ions requires either to use fluorescent functional monomers or to embed with IIPs fluorescence substances like quantum dots ~~with IIPs~~ [23–26]. This latter solution is associated with a quenching of the fluorescence in the presence of the target, whereas the use of fluorescent monomers offers both the on-off (quenching) and off-on (enhancement) mode. The sensitivity is usually

increased with the off-on mode because of an absence of fluorescent background and a high signal-to-noise ratio [24]. Up to now, the development of fluorescent IIP based on an exaltation of the signal upon metal ion binding is limited to Hg(II), Al(III), Ag(I), Zn(II) and Cd(II) [27–31].

In a previous study, we reported the preparation of a fluorescent functional monomer, ANQ-ST, for the chelation of Pb(II) with an off-on selective fluorescence answer [32]. ANQ-ST was specially designed by the association of a fluoroionophore combining 5-amino-8-hydroxyquinoline and anthracene, as a ligand for Pb(II) and a fluorescent dye, respectively, with a styrene moiety as a polymerizable group. ANQ-ST was copolymerized with ethylene glycol dimethacrylate (EGDMA) to prepare an IIP for Pb(II) [33]. The obtained results proved the efficiency of such an IIP based on ANQ-ST for Pb(II) detection by fluorescence. In the present work, we explore different polymerization solvent mixtures, different functional monomer contents and another crosslinker, divinylbenzene (DVB), to evaluate their impact on the IIP properties. Before performing the polymerization step, we studied in detail the self-assembly step between Pb(II) and ANQ-ST. ~~The aim of t~~ This preliminary investigation ~~was~~ aimed to optimize the stoichiometry of the complex formed between Pb(II) and ANQ-ST in the polymerization conditions (temperature and solvent). The synthesized IIPs were then characterized and the influence of their composition onto the recovered fluorescence signal was assessed and validated in various media, including natural waters.

2. Materials and methods

2.1. Reagents and instruments

$AgNO_3$, $CaCO_3$, $ZnSO_4$ and $NaNO_3$ were purchased from Fisher Scientific (Analytical grade), $CdSO_4$, $Co(NO_3)_2$ and $CuSO_4$ from Merck (pro analysis grade), $Pb(NO_3)_2$ from Carlo Erba (Analytical grade). Ethylene glycol dimethacrylate (EGDMA) was purchased from Fischer Scientific (98%, contains 90-110 ppm monomethyl ether hydroquinone as inhibitor), methyl methacrylate (MMA) from Merck (99%, contains 30 ppm MEHQ as inhibitor), divinylbenzene (DVB) from Merck (80%, contains 20% of ethylvinylbenzene) and azobisisobutyronitrile (AIBN) from Merck (98%), ethylenediaminetetraacetic acid (EDTA) from Merck (99%), 4-(2-hydroxyethyl)-1-piperazineethanesulfonic acid (HEPES buffer) from Fischer Scientific (99%). Solvents were purchased from Fischer Scientific (reagent grade). Dry solvents were purchased as extra dry grade (Fischer Scientific).

UV-visible absorption spectra were recorded with a Shimazu UV-2501 spectrophotomer. ^{13}C CP-MAS NMR spectra were obtained with Bruker Avance 400 MHz Ultrashiel spectrometer at 100 MHz with magic angle spinning (MAS) frequency $\omega r/2\pi = 10$ kHz. Scanning Electron Microscopy (SEM) images were taken with Supra40 VP microscope. Surface areas and pore volumes were determined by nitrogen

adsorption/desorption experiments on a volumetric adsorption analyser Quantachrome Nova2200e (Quantachrome Instruments USA), at liquid nitrogen temperature. The BET model was applied for surface area determination and the BJH method was used for pore size determination. Inductively coupled plasma mass spectrometry ICP-MS (NexION® Series 300) was used for metals concentration determination. The Excitation-Emission Matrices (EEMs) of fluorescence were recorded on a HITACHI F4500 spectrofluorimeter. The excitation wavelength ranged from 320 to 460 nm, with a step of 10 nm and an excitation slit of 1 nm. The corresponding emission spectra were acquired from 350 to 550 nm with a scan speed of 2400 nm.min−1 and a slit of 1 nm. The photomultiplicator tension was fixed at 950 V and the integration time set at 0.1 s. The extraction of the 5 nm stepped emission was obtained by FL-Solution software. All the EEM of fluorescence were cleaned from the diffusion signals: Rayleigh by cutting the diffusion band (20 nm) and Raman from first and second order by applying Zepp procedure [34].

2.2. Pb(II) and functional monomer ANQ-ST distribution modelling from UV-visible spectra

The functional fluorescent monomer ANQ-ST was prepared according to our previous study [32]. Pb(II) complexation with ANQ-ST was studied at 80°C, the temperature of polymerization, in different solvents: DMSO, DMSO-MeOH (1:1, v-v) and DMSO-ACN(1:1, v/v). The experiments were carried out in 3 mL quartz Suprasil® cells. The combined concentration of Pb(II) (0-0.1 mmol.L^{-1}) and ANQ-ST (0-0.1 mmol.L^{-1}) was kept constant (0.1 mmol.L^{-1}), but the ratio ligand/Pb(II) ~~was varied~~ ranged from 0.1 to 10 using $Pb(NO_3)_2$ as Pb(II) source. 14 spectra were recorded using UV-vis spectrometer. At equilibrium, the distribution of the various species (free metal, 1:1 complex, 1:2 complex, 1:3 complex and free ligand) was calculated using a commercial program (HypSpec) based on the least-squares minimization scheme [35,36]. Stability constants, extinction coefficients and concentrations of all absorbing components were simultaneously estimated. The extinction coefficients for uncomplexed Pb(II) were determined from independent measurements.

2.3. Synthesis of fluorescent Pb(II)-IIPs particles

The ion-imprinted polymers (IIPs) and non-imprinted polymers (NIPs) were prepared by precipitation polymerization. Initially, for IIPs particles, the functional monomer ANQ-ST was dissolved in 20 mL of DMSO-MeOH (1:1, v/v) mixture in a 120 mL cylinder-shaped Pyrex tube (compositions are given Table 1). $Pb(NO_3)_2$ was added and the solution was stirred for 30 min. Following, the crosslinker (EGDMA or DVB) and MMA (for IIPB) was added and the solution was gently flushed with argon for 15 min. The initiator (AIBN) was added to the above mixture and the solution was flushed again with argon for 5 min. The tube was placed in a hybridation oven (HB-100 Hybridizer from UVP, UK) preheated at 30°C and rotated at 8 rpm. The temperature of the oven was increased from 30 to 80°C with a ramp of 5°C every 15 min. After 24 h of polymerization, the obtained particles were sequentially

washed using DMSO, dichloromethane and acetone to remove the residual monomers. Then, to remove the template ion Pb(II), the particles were introduced in Corning® tubes with 20 mL of 0.1 mol.L^{-1} EDTA solution. After 2 h of stirring and 2 h in an ultrasonic bath, the polymer was filtered. To check the efficiency of the procedure, the Pb content in the filtrate was controlled by ICP-MS. Before the analysis, 20 µL of pure nitric acid was added to the filtrate to prevent any precipitation. This washing step procedure was repeated until Pb(II) concentration in the filtrate was close to the detection limit of ICP-MS. Eventually, the polymer was ground to disperse the particles and dried under vacuum overnight. NIPs particles were synthesized following the same procedure in the absence of the lead template ions.

Table 1. *Composition of the prepared polymers*

		IIPA	***NIPA***	***IIPB***	***NIPB***	***IIPC***	***NIPC***
$Pb(NO_3)_2$ (mmol)		0.21	–	0.085	–	0.15	–
ANQ-ST (mmol)		0.50		0.20		0.35	
Crosslinker (mmol)	EGDMA	8.40		9.75		–	
	DVB	–		–		17.25	
MMA (mmol)		–		0.30		–	
AIBN (mmol)		0.25		0.25		0.30	
Molar ratio ANQ-ST/monomers (%)		5.6		2.0		2.0	

2.4. Binding isotherms / Adsorption of Pb(II)

Batch experiments were carried out for Pb(II) adsorption studies. 10 mg of IIP or NIP was put in contact with 10 mL of Pb(II) buffered solution (pH = 6.0, HEPES buffer) of various concentration ~~of~~ (0-60 mg.L^{-1}) into 15 mL Corning® tube. After 24 h of stirring and adsorption equilibrium, the polymer was filtered. 10 µL of pure nitric acid was added to the filtrate to prevent any precipitation. The equilibrium concentration (C_e) of Pb(II) was determined by ICP-MS. Pb(II) adsorption capacity of IIP or NIP was calculated by the following equation:

$$Q = \frac{(C_0 - C_e) * V}{m}$$

With C_0 and C_e the initial and the equilibrium concentration of Pb(II), V the volume of solution and m the weight of IIP or NIP.

2.5. Fluorescence measurements

For all the fluorescence measurements, 3 mg of polymer were suspended in 3 mL of solvent in a quartz cuvette and the fluorescence was measured after 24h of stirring.

In a first step, the selectivity was measured in a water-acetone (1:4, v/v) mixture by adding 241 nmol.L^{-1} of Ag(I), Na(I), Ca(II), Cd(II), Co(II), Cu(II), Pb(II) or Zn(II) to the polymer suspension in the quartz cuvette. In a second step, the fluorescence of the polymers was measured in water-acetone (1:4, v/v) mixture in the presence of 241 nmol.L^{-1} Pb(II) and 1, 2 or 10 equivalents of interfering ions (Ag(I), Na(I), Ca(II), Cd(II), Co(II), Cu(II) or Zn(II)).

The fluorescence of the polymers was studied in different media: pure water, water-acetone (1:4, v/v) mixture, buffered water (HEPES buffer) at pH =7.0 and 8.1, tap water (sampled in Toulon, France) and seawater (sampled in Toulon harbour, France). The last two samples were filtered before use (0.2 µm syringe filters, cellulose nitrate, Sartorius®). Increasing amounts of Pb(II) were added to the cuvette containing the polymer in suspension. After 24 h of stirring, the fluorescence signal was measured. ~~A~~ The addition of Pb(II) was repeated to obtain the complete range (0-100 µg.L^{-1}).

Validation of lead determination was achieved in different water samples filtered before use (0.2 µm syringe filters, cellulose nitrate, Sartorius®): tap water (sampled in Toulon), mineral water (Evian®) and seawater (sampled in Toulon harbour). 10 µg.L^{-1} of Pb(II) was added to the studied waters before measurements. After 24 h of stirring, the fluorescence was measured with 3 replicates.

3. Results and discussions

3.1. Optimization of the metal/ligand ratio in the polymerization conditions

The role of the functional monomer is fundamental in the preparation of IIPs because it ensures the formation of a coordination complex with the target ion ~~that will~~ further ~~be mainly~~ responsible for the selectivity of the IIP. This formation step is crucial on two aspects: the chemical structure of the monomer, *i.e.* its intrinsic chelating properties, and the stoichiometry of the complex with the metal ion. In previous studies, we reported that it was possible to precisely adjust this stoichiometry in the pre-polymerization mixture in order to select a 1:2 or 1:3 metal:ligand complex [37]. The IIPs obtained in ~~those~~ these conditions were as efficient as ~~those~~ that prepared with a previously-isolated complex ~~prepared~~ obtained by *ex-situ* precipitation [38]. The advantage of this selection method is to optimize the formation of the complex without performing the tedious steps necessary for the *ex-situ* complex isolation.

In the present work, the complexation of Pb(II) with the functional monomer ANQ-ST was studied at 80°C, *i.e.* the polymerization temperature. The objective was to determine the exact proportions of ANQ-ST and Pb(II) that will optimize the formation of the coordination complex in the pre-polymerization conditions. Three different reaction media (solvent or mixtures of solvents) allowing to dissolve the monomer and the Pb(II) salt were tested: DMSO, DMSO-MeOH (1:1, v/v) and DMSO-ACN (1:1, v/v). A collection of UV-visible adsorption spectra of solutions containing Pb(II) and ANQ-ST were recorded by keeping the overall concentration of Pb(II) and ANQ-ST constant while varying their molar ratio. Fig.1 presents the distribution of each complex as a fraction of the total distribution.

This clearly shows that, whereas the 1:3 complex is never predominant, it is possible to isolate the 1:2 complex, $Pb(ANQ\text{-}ST)_2$, by carefully adjusting the initial Pb(II)/ANQ-ST ratio. These optimum conditions are given in Table 2 as being 0.47, 0.42 and 0.47 for DMSO, DMSO-MeOH (1:1, v/v) and DMSO-ACN (1:1, v/v) respectively. It can also be noted that the standard conditions for preparing a 1:2 complex (ratio of 0.5) lead to a lower proportion of 1:2 complex compared to the 1:1 complex. This is especially true in the case of the DMSO-MeOH mixture. Finally, the high values of all the constants of formation of the complex reported in Table 2 proved that the complex formation reactions can be considered as total.

Table 2. *Constants of formation of the complex formed by Pb(II) and ANQ-ST in different solvents at 80°C and composition of the solution depending on Pb/ANQ-ST ratio*

Solvent	***Constants of formation***			***Composition of the solution depending on Pb/ANQ-ST ratio (molar fraction)***				
	Log(β1)	***Log(β2)***	***Log(β3)***	**$[Pb^{2+}]/[ANQ\text{-}ST]$**	**Free ANQ-ST**	**1:1 Complex**	**1:2 Complex**	**1:3 Complex**
DMSO	8.03	15.23	19.44	0.47	2 %	2 %	94 %	2 %
				0.50	1 %	8 %	90 %	1 %
DMSO-MeOH (1:1, v/v)	7.28	13.71	17.41	0.42	5 %	4 %	90 %	1 %
				0.50	3 %	13 %	84 %	1 %
DMSO-ACN (1:1, v/v)	6.32	13.63	17.68	0.47	3 %	2 %	94 %	2 %
				0.50	2 %	5 %	92 %	1 %

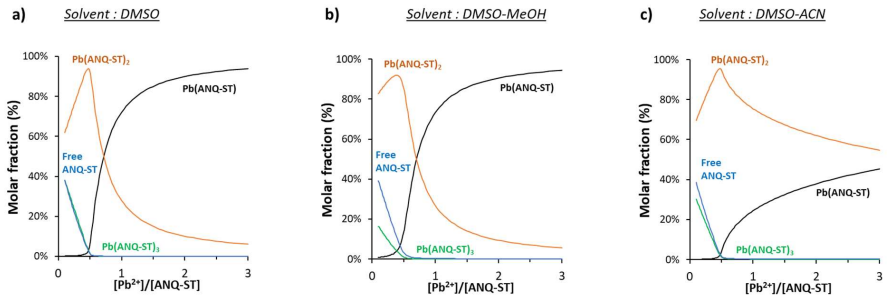

Fig. 1. *Metal and ligand species distribution calculated from UV-visible spectra using HypSpec program [35,36] for lead and ANQ-ST at 80°C. Solvent: a) DMSO, b) DMSO-MeOH (1:1, v/v), c) DMSO-ACN (1:1, v/v).*

3.2. Synthesis of the Pb(II)-IIPs

In order to obtain the fluorescent IIPs as particles, precipitation polymerization was carried out. Indeed, this technique, commonly used to develop imprinted polymers, ~~makes it possible~~ allow to prepare particles of submicrometric to micrometric size ~~that are~~ easily ~~to~~ recovered by filtration or centrifugation [39]. Thus, the grinding step required to obtain particles after bulk polymerization is not necessary, which avoids a laborious step leading to the loss of a large quantity of polymer. One of the major difficulties to perform this apparently simple process is to find the good solvent that will solubilize the monomers and the target but precipitate the polymers during their formation. Despite many attempts in which we varied the ratio of the amounts of functional monomer/crosslinker and the ratio of the total amount of monomers/solvent, we failed to obtain IIP particles with DMSO and with the DMSO-ACN (1:1, v/v) mixture. Therefore, only the DMSO-MeOH (1:1, v/v) mixture allowed preparing IIPs and their corresponding non-imprinted polymers (NIPs) as particles by precipitation polymerization. However, it required to increase the mass ratio of the total amount of monomers/solvent up to 10%, far above the usual 2 to 3% ratio.

In addition to EGDMA, which is the most classical crosslinker to prepare IIPs, we also used DVB in order to give more rigidity to the polymer matrix. It is established that the formation of stable particles by precipitation polymerization strongly depends on the degree of crosslinking and that this technique requires a high level of crosslinker [40]. In the case of ANQ-ST, a minimum molar fraction of 94.4% of EGDMA crosslinker was necessary to obtain IIP particles (IIPA) and a minimum of 98% of DVB was required (IIPC) (Table 1). IIPB was prepared with a similar molar fraction of EGDMA crosslinker (95%) as IIPA but with less functional monomer ANQ-ST (2%). The difference was replaced with 3% molar fraction of MMA, a neutral co-monomer (Table 1).

The fluorescent IIPs based on ANQ-ST were prepared as depicted in the synthesis scheme shown in Fig.2.a. The optimal ratio $[Pb^{2+}]/[ANQ\text{-}ST]$ of 0.42, previously determined, was used for the synthesis of the IIPs. IIPA, IIPB and IIPC were obtained as yellow-orange powders (Fig.2.b) with a yield of 93%, 57% and 66%, respectively. The corresponding non-imprinted polymers (NIPs) were prepared with the same procedure in the absence of Pb(II). NIPA, NIPB and NIPC were obtained as yellow powders (Fig.2.b) with a yield of 98%, 89% and 93%, respectively. The difference of colour between the IIPs and corresponding NIPs is explained by the absence of Pb(II) template ions in the NIPs.

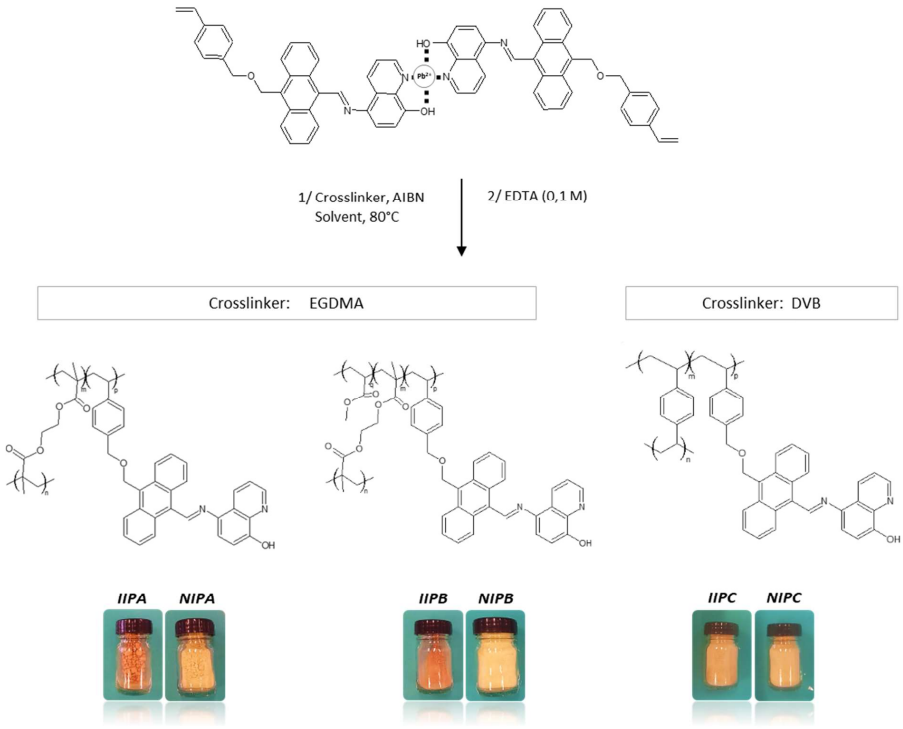

Fig.2. *Synthesis route of Pb(II)-IIPs and pictures of the synthesized IIPs (before Pb(II) extraction) and NIPs.*

3.3. Characterization of the chemical structure of Pb(II)-IIPs

In order to confirm the integration of the functional monomer ANQ-ST in the polymer matrices, solid-phase ^{13}C CP-MAS NMR spectra were recorded. Fig.3.a shows the spectra of poly(EGDMA), IIPs and their corresponding NIPs synthesized with EGDMA as the crosslinker. All polymers showed the characteristic peaks of the poly(EGDMA) structure: 185.1 ppm for the carbonyl of the ester function, 70.7 ppm for the carbons bound to the ether oxygen (-O-CH_2-CH_2-O-). The peaks at 53.5, 31.9 and 28.2 ppm were respectively assigned to quaternary, methylene (-CH_2-) and methyl (-CH_3) carbons of the polymer chains. The presence of the peaks at 144.6 and 134.5 ppm, assigned to the aromatic carbons of the styrene, anthracene and 5-amino-8-hydroxyquinoline moieties of ANQ-ST, proved the correct integration of the ANQ-ST monomer in the IIPs and NIPs. This is in ~~accordance~~ agreement with the yellow to the orange colour of these polymers due to the coloured functional monomer, whereas ~~as~~ poly(EGDMA) or poly(DVB) are white polymers.

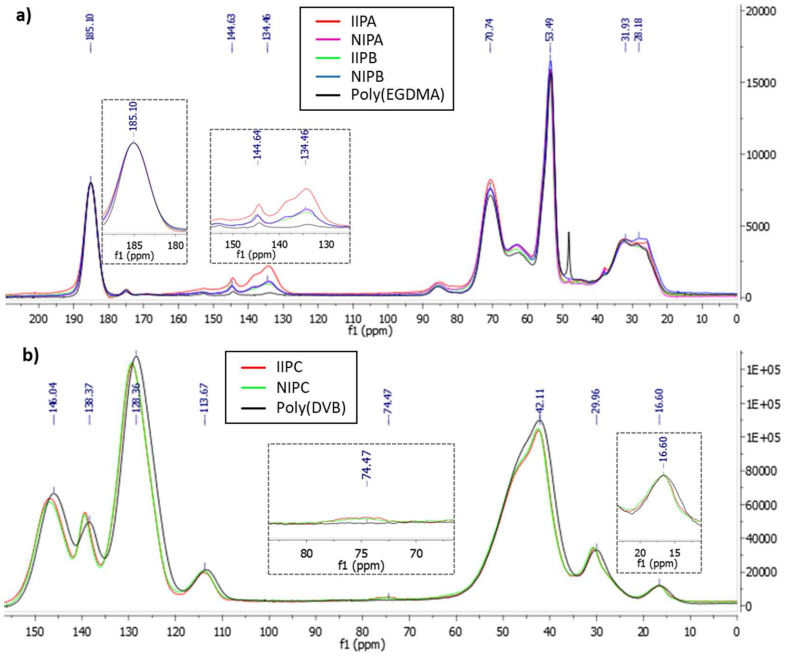

Fig.3. *^{13}C MAS NMR spectra of the polymers synthesized with a) EGDMA or b) DVB as crosslinker.*

Fig.3.b shows the ^{13}C CP-MAS NMR spectra of poly(DVB), IIPC and its corresponding NIP synthesized with DVB as the crosslinker. They present the characteristic signals of the poly(DVB) back-bone: peaks at 146.0 and 128.4 ppm of the quaternary and tertiary aromatic carbons and peaks at 138.4 and 113.7 ppm of the tertiary and secondary vinylic carbons, respectively (from non-polymerized vinyl groups). The large peak at 42 ppm was assigned to the carbon backbone of the polymers (-CH_2-CH-) and the signals at 30.0 and 16.6 ppm were assigned to the ethyl groups of the ethylvinylbenzene contained in the commercial DVB (pure at 80%). The incorporation of the functional monomer was assessed by the signal at 74.5 ppm, assigned to the carbon bound to the oxygen and to the styrenic cycle of ANQ-ST. ~~Because of~~ Due to the aromatic structure of the DVB, it was more difficult to evidence the incorporation of ANQ-ST by ^{13}C CP-MAS NMR. Nevertheless, in addition to the weak signal at 74.5 ppm, the yellowed colour of IIPC and NIPC after washing can also be considered as ~~a~~ proof of the presence of ANQ-ST in the polymer matrix.

3.4. Characterization of the morphology of Pb(II)-IIPs

Scanning electron microscopy (SEM) reveals that the nature of the crosslinker has a real impact on the morphology of the polymers (Fig.4.a). Indeed, on the SEM pictures of the polymers synthesized with

EGDMA, aggregated nano-sized particles with diameters in the range of 30 to 100 nm could be observed. On the other hand, polymers synthesized with DVB as the crosslinker consisted of aggregated particles in the range of 600 nm to 2 µm. NIPC particles were almost spherical and IIPC presented more irregular shapes. The type of morphology of the various polymers is commonly observed in the literature for the synthesis of IIPs by precipitation polymerization [41–44].

The polymers porosity was studied by nitrogen adsorption/desorption experiments (Fig.4.b). Such measurements could not be performed for IIPB due to an insufficient quantity of polymer. Nevertheless, the result should be similar to that of IIPA because of the close morphology observed in the SEM experiments and of the similar fraction of crosslinker. Except for NIPC, all the isotherms can be classified as type IV according to the IUPAC classification [45]. This category of isotherm is characteristic of mesoporous materials with pores diameters varying from 2 to 50 nm. This is in ~~accordance~~ agreement with the pore sizes determined by the BJH method: 7.4, 6.6, 4.7 and 3.9 nm for IIPA, NIPA, NIPB and IIPC, respectively. Moreover, the forms of hysteresis loops with parallel adsorption and desorption branches are typical of materials with narrow pores distribution. The isotherm of NIPC is of type I, characterizing materials containing micropores, with a good correlation with the value of 2.1 nm determined for the pore size. The pore size measured for the polymers prepared with EGDMA appears to be bigger than those obtained for polymers synthesized with DVB, as a possible result of the rigidity induced by DVB. All the polymers showed high surface areas of 325, 401, 363, 422 and 452 $m^2.g^{-1}$ for IIPA, NIPA, NIPB, IIPC and NIPC, respectively.

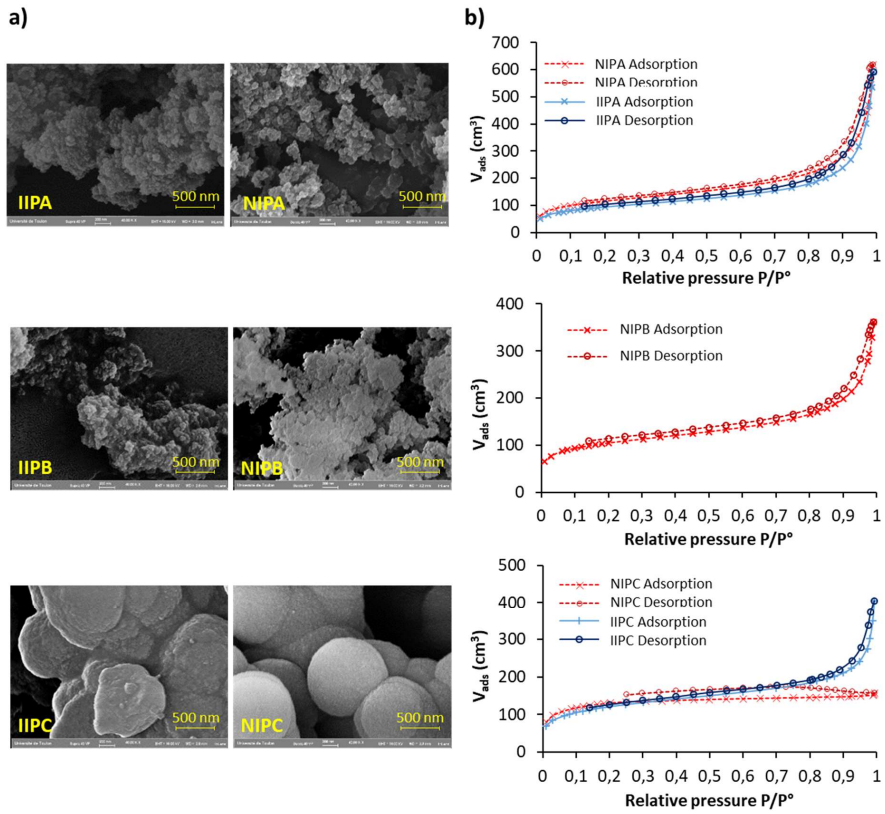

Fig.4. *a) Scanning electron microscopy pictures for IIP and NIP and a) Nitrogen adsorption/desorption isotherms of the prepared IIP and its corresponding NIP.*

3.5. Impact of the Pb(II)-IIPs composition on their binding properties

The impact of the composition of the IIPs was evaluated through fluorescence measurements. In the preliminary study of ANQ-ST, we showed that this polymerizable fluoroionophore answers in a "turn-on" mode to the presence of Pb(II) [32]. Its relative fluorescence signal linearly increased upon Pb(II) addition before reaching saturation. The fluorescence of all the prepared polymers in the presence of different concentrations of Pb(II) (from 0 to 100 µg.L^{-1}) was measured in water-acetone (1:4, v/v) mixture. The results showed that for IIPA and IIPB, synthesized with EGDMA as crosslinker, the relative fluorescence intensity linearly increased up to 60-70 µg.L^{-1} (Fig.5.a and Fig.5.b). For IIPA, prepared with 5.6% of ANQ-ST, the slope of the calibration curve was found to be higher than that of NIPA, as a result of ~~an~~ the imprinting effect (Fig.5.a). An imprinting factor of 2.93, calculated as the IIP

calibration curve slope divided by that of the NIP, was found. For the polymers synthesized with 2% of ANQ-ST, the slope of the calibration curve of NIPB was higher than that of IIPB (Fig.5.b). This prevents the further use of IIPB in the present study.

While using DVB as crosslinker, the variation of the fluorescence intensity was not significant for IIPC (Fig.5.c). For both IIPC and NIPC, the fluorescence signal did not present any clear trend. From the observations carried out during the experiments, we attribute these incoherent results to a wettability problem. Indeed, DVB is a more hydrophobic monomer than EGDMA and its fraction in IIPC and NIPC is so high that it makes those polymers slightly wettable. This limits the application of those polymers for the quantification of Pb(II). Thus, taking into account the results obtained for IIPB and IIPC, the rest of the present study was solely dedicated to IIPA.

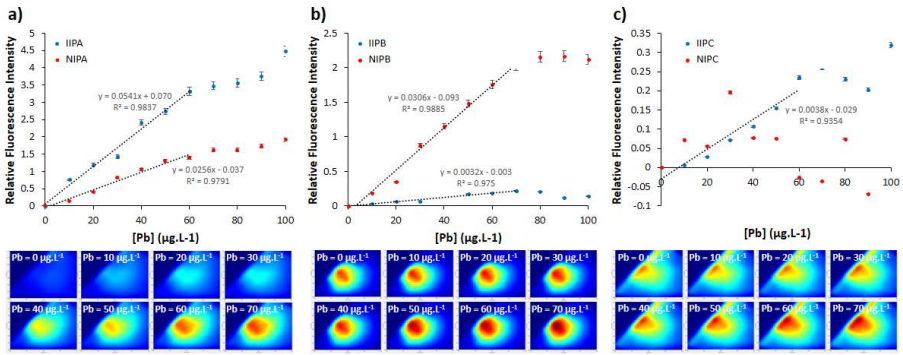

Fig.5. *Relative fluorescence intensity $(I-I_0)/I_0$ of IIP and NIP versus the concentration of Pb(II) and the corresponding EEMs of IIP in water-acetone (1:4, v/v); with I the fluorescence intensity at a given concentration of Pb(II) and I_0 the intensity in the absence of Pb(II). a) IIPA / NIPA with $(\lambda_{em}/\lambda_{ex})$ = 380/445 nm for IIPA and $(\lambda_{em}/\lambda_{ex})$ = 395/430 nm for NIPA, b) IIPB / NIPB with $(\lambda_{em}/\lambda_{ex})$ = 395/425 nm for IIPB and NIPB, c) IIPC / NIPC with $(\lambda_{em}/\lambda_{ex})$ = 405/435 nm for IIPC and $(\lambda_{em}/\lambda_{ex})$ = 390/420 nm for NIPC.*

3.6. Study of Pb(II)-IIP selectivity by fluorescence

In a first step, the fluorescence responses of IIPA and NIPA were studied in a water-acetone (1:4, v/v) mixture in the presence of a single ion species: Pb(II), Ag(I), Na(I), Ca(II), Cd(II), Co(II), Cu(II) or Zn(II) (Fig.6.a), chosen as water major ions or competitors for the binding cavities. The corresponding Excitation-Emission Matrices (EEMs) of fluorescence, and the further quantifications through the determination of the relative fluorescence intensity, clearly showed that IIPA was very sensitive to the presence of Pb(II) ions and almost not to that of the other ions. Thus, in the case of Pb(II), the fluorescence increases by 312% compared to the reference signal of IIPA. Zn(II) also induced an increase of the fluorescence signal but to a much less extent than Pb(II). On the other hand, the signal of NIPA differently evolved ~~in a different way~~ with an important impact of all the ions. The imprinting effect is therefore clearly evidenced (i) by the comparison with the lower signal of NIPA compared to

that of IIPA in the presence of Pb(II), with an imprinting factor of 2.4, and (ii) by the more important impact of most of the interfering ions on the NIPA signal. ~~The best result is obtained~~ This observation is especially true for Ca(II) with a close to zero value for IIPA compared to an increase of 70% of the relative fluorescence intensity for NIPA.

To highlight the selectivity of the IIP, the fluorescence of IIPA and NIPA was also studied in the presence of Pb(II) mixed with one or two equivalents of an interfering ion species (Ag(I), Na(I), Ca(II), Cd(II), Co(II), Cu(II) or Zn(II)) (Fig.6.b). Due to their high presence in aqueous media like mineral water or seawater, the addition of ten equivalents of Na(I) and Ca(II) was also tested. In these experiments, the reference intensity is that of the polymer in presence of one equivalent of Pb(II) alone. The results showed that the impact of the addition of one or two equivalents of interfering ions on the fluorescence intensity of IIPA and NIPA is limited. As far as Na(I) and Ca(II) are concerned, their presence at a very high concentration compared to that of lead (10 equivalents) did not seem to impact much the response of IIPA, demonstrating its selectivity. These encouraging results converge on a promising use of IIPA as a sensing material for Pb(II) in real waters samples.

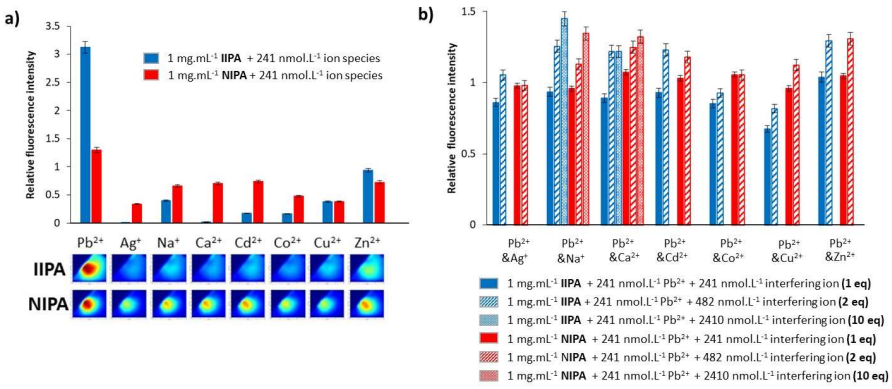

Fig.6. *Relative fluorescence intensity $(I-I_0)/I_0$ of IIP and NIP in water-acetone (1:4, v/v). a) with I_0 the fluorescence intensity of IIPA / NIPA and I the fluorescence intensity of IIPA / NIPA in the presence of an ion species (241 nmol.L^{-1} of Pb(II) = 5 mg.L^{-1}) with $(\lambda_{em}/\lambda_{ex})$ = 380/445 nm for IIPA and $(\lambda_{em}/\lambda_{ex})$ = 395/430 nm for NIPA. b) with I_0 the fluorescence intensity of IIPA / NIPA in the presence of Pb(II) alone and I the fluorescence intensity of IIPA / NIPA in the presence of Pb(II) and an interfering ion, with $(\lambda_{em}/\lambda_{ex})$ = 380/445 nm for IIPA and $(\lambda_{em}/\lambda_{ex})$ = 395/430 nm for NIPA.*

3.7. Determination of Pb(II) by IIPA in pure and real water samples

The adsorption capacities of the IIPA and its corresponding NIP for Pb(II) were investigated in batch experiments. Fig.7.a shows the adsorbed Pb(II) amount depending on the initial concentration of Pb(II) in solution. Maximum adsorption capacities of IIP and NIP for Pb(II) were 4.5 and 2.6 mg.g^{-1}, respectively. An imprinting factor of 1.7, calculated as the adsorption capacity of the IIP ~~on~~ divided by that of the NIP, was obtained.

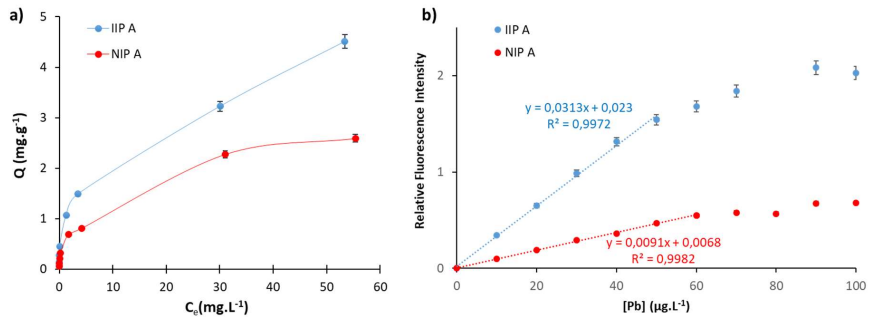

Fig.7. *a) Adsorption isotherms of Pb(II) ions of IIPA and NIPA and b) Calibration curves in ultra-pure water (pH = 5.9) plotting the relative fluorescence intensity ($I-I_0$)/I_0 of IIPA / NIPA versus the concentration of Pb(II) with ($\lambda_{em}/\lambda_{ex}$) = 380/445 nm, I the fluorescence intensity at a given concentration of Pb(II) and I_0 the intensity in the absence of Pb(II).*

The adsorption isotherms were processed with Langmuir and Freundlich models, the most used linearization models. Langmuir assumes that adsorption occurs through homogenous and equivalent adsorption sites whereas Freundlich postulates that adsorption occurs on multi-layer heterogenous surface [46,47]. IIPA adsorption was best linearized using Freundlich model (R^2 = 0.95) whereas NIPA adsorption was best fit using Langmuir (R^2 = 0.96). These results demonstrated that imprinting leads to ~~the~~ heterogenous adsorption through the creation of specific cavities for Pb(II) along with non-specific sites. Concerning NIP, the absence of any selective cavities leads to ~~a~~ homogenous distribution of non-specific sites, with equivalent adsorption properties.

The evolution of the relative fluorescence intensity as a function of Pb(II) concentrations present a similar linear variation up to 50 µg/L for both IIPA and NIPA. However, the calibration curve of IIPA presents a slope more than 3 times higher than that of NIPA, again demonstrating the positive impact of the imprinting effect (Fig.7.b). Thereby, an imprinting factor of 3.4 can be calculated as the ratio of the slopes of the calibration curves of IIPA and NIPA. The limit of detection, calculated as the amount of Pb(II) that increased three times the standard deviation of the blank signal [48,49], was much more

interesting in the case of IIPA: 2.4 µg/L compared to 11 µg/L for NIPA, leading to linear ranges of 8.0-50 µg/L and 36.7-50 µg/L, respectively. Concerning IIPA, when comparing these values to regulations specific for Europe [12], USA [13] and WHO, the specialized agency of the United Nations responsible for international public health [50], it is clear that the presented material perfectly fits all the regulations: 7.2 µg/L [12], 15 µg/L [13] and 10 µg/L [50], respectively.

To evaluate the effect of different matrices and pH on IIPA fluorescence properties, calibration curves were also recorded in the presence of different concentrations of Pb(II) (from 0 to 50 $\mu g.L^{-1}$) in buffered water (pH = 7.0 and 8.1), seawater (pH = 7.9) and tap water (pH = 7.6). The slopes of the obtained calibration curves appeared to be very close (Fig.8) meaning that the wide range of studied pH and matrices has a little impact on the fluorescence detection of Pb(II) by IIPA. For the various matrices, the limit of detection (LOD) was found to be 2.4 $\mu g.L^{-1}$, similar to that in ultra-pure water, proving that IIPA remains very ~~effective~~ efficient whatever the matrix and the pH.

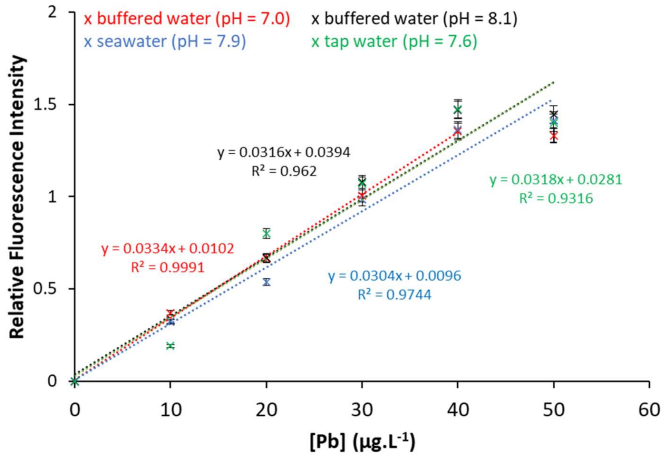

Fig.8. *Calibration curves plotting the relative fluorescence intensity $(I-I_0)/I_0$ of IIPA versus the concentration of Pb(II) in different matrices with $(\lambda_{em}/\lambda_{ex})$ = 380/445 nm, with I the fluorescence intensity at a given concentration of Pb(II) and I_0 the intensity in the absence of Pb(II).*

IIPA was then tested for the detection of Pb(II) in real water samples. Tap water, mineral water and seawater samples were spiked with 10 $\mu g.L^{-1}$ of Pb(II). The previously obtained calibration curves were used to determine~~d~~ Pb(II) concentration in the spiked samples. Good recovery rates in the range of 96-113% were obtained (Table 3). Results emphasized the potential for IIPA to detect Pb(II) in natural waters.

Table 3. *Determination of Pb(II) in different water samples*

Sample	*Spike ($\mu g.L^{-1}$)*	*Found ($\mu g.L^{-1}$)*	*Recovery (%)*
Tap water (Toulon city, France)	10.0	11.3 ± 0.1	113
Mineral water (Evian®)	10.0	11.0 ± 1.1	110
Sea water (Toulon harbor, France)	10.0	9.6 ± 1.9	96

4. Conclusions

The present study focuses on the elaboration of a fluorescent IIP for Pb(II) based on a fluorescent styrenic monomer, ANQ-ST. In a preliminary study performed in the conditions of the polymerization (temperature and solvent), the ratio between Pb(II) and ANQ-ST was optimized to selectively prepare a complex with a 1:2 stoichiometry. Then, IIPs were synthesized by precipitation polymerization with either EGDMA or DVB as crosslinkers. Precipitation polymerization is a very practical method to prepare IIPs as particles. Unfortunately, due to its own principle, it is very sensitive to the thermodynamical compatibility between the used monomers and the polymerization solvent. Therefore, in ~~those~~ these conditions, only the DMSO-MeOH (1:1, v/v) solvent mixture was suitable to solubilize the Pb(II) salt and the monomers and to precipitate the IIP. Moreover, it was not possible to incorporate more than 5.6% and 2% of ANQ-ST in IIPs and NIPs prepared with EGDMA and DVB, respectively. The use of DVB was explored because of the potential rigidity that it could introduce in the polymer matrix, which could positively affect the imprinting effect. Nevertheless, the association of the two hydrophobic monomers, ANQ-ST and DVB, lead to polymers with too low wettability properties. In ~~those~~ these conditions, their use as chemical sensor for Pb(II) in aqueous media appeared to be too limited. As far as EGDMA was concerned, IIP and NIP were prepared with 5.6 and 2% of functional monomer, while keeping the crosslinker fraction constant, not to impact the morphology of the IIPs. The best results were obtained with IIPA, based on 5.6% on ANQ-ST.

This IIPA was further studied for the detection of Pb(II) by fluorescence. It gave good results in terms of selectivity towards interfering ions Ag(I), Na(I), Ca(II), Cd(II), Co(II), Cu(II) and Zn(II), even in competing mode with some of these ions introduced in moderate to important excess. It was also proved that IIPA was slightly sensitive to the pH and the nature of the aqueous matrix by the comparison of calibration curves obtained in different types of waters and at different pH: ultra-pure water (pH = 5.9), buffered waters (pH = 7.0 and 8.1), tap water and seawater. This was confirmed by the successful determination of Pb(II) in some real sample waters. All these promising results, associated with the low limit of detection within ranges recommended by the legislation of various countries, validate this fluorescent IIP as a potential sensing material for Pb(II) easy quantification.

Acknowledgements

This work was financially supported by PREVENT research program (funded by the University of Toulon, Toulon-Provence-Méditerranée (TPM) and the Conseil Départemental du Var, France) and by the Regional Council of Provence Alpes Côte d'Azur (France).

References

[1] S.T. Shefa, P. Héroux, Both physiology and epidemiology support zero tolerable blood lead levels, Toxicol. Lett. 280 (2017) 232–237. https://doi.org/10.1016/j.toxlet.2017.08.015.

[2] J.E. Towner, T.A. Pieters, P.K. Maurer, Lead Toxicity From Intradiscal Retained Bullet Fragment: Management Considerations and Recommendations, World Neurosurg. 141 (2020) 377–382. https://doi.org/10.1016/j.wneu.2020.05.112.

[3] A.L. Wani, G.G. Hammad Ahmad Shadab, M. Afzal, Lead and zinc interactions – An influence of zinc over lead related toxic manifestations, J. Trace Elem. Med. Biol. 64 (2021) 126702. https://doi.org/10.1016/j.jtemb.2020.126702.

[4] M.P. Taylor, P.J. Davies, L.J. Kristensen, J.L. Csavina, Licenced to pollute but not to poison: The ineffectiveness of regulatory authorities at protecting public health from atmospheric arsenic, lead and other contaminants resulting from mining and smelting operations, Aeolian Res. 14 (2014) 35–52. https://doi.org/10.1016/j.aeolia.2014.03.003.

[5] D.H. Dang, J. Schäfer, C. Brach-Papa, V. Lenoble, G. Durrieu, L. Dutruch, J.-F. Chiffoleau, J.-L. Gonzalez, G. Blanc, J.-U. Mullot, S. Mounier, C. Garnier, Evidencing the Impact of Coastal Contaminated Sediments on Mussels Through Pb Stable Isotopes Composition, Environ. Sci. Technol. 49 (2015) 11438–11448. https://doi.org/10.1021/acs.est.5b01893.

[6] D. O'Connor, D. Hou, J. Ye, Y. Zhang, Y.S. Ok, Y. Song, F. Coulon, T. Peng, L. Tian, Lead-based paint remains a major public health concern: A critical review of global production, trade, use, exposure, health risk, and implications, Environ. Int. 121 (2018) 85–101. https://doi.org/10.1016/j.envint.2018.08.052.

[7] P. Jarvis, J. Fawell, Lead in drinking water – An ongoing public health concern?, Curr. Opin. Environ. Sci. Health. 20 (2021) 100239. https://doi.org/10.1016/j.coesh.2021.100239.

[8] O.E. Orisakwe, J.K. Nduka, Lead and cadmium levels of commonly administered pediatric syrups in Nigeria: a public health concern?, Sci. Total Environ. 407 (2009) 5993–5996. https://doi.org/10.1016/j.scitotenv.2009.08.033.

[9] J.E. Forsyth, S. Nurunnahar, S.S. Islam, M. Baker, D. Yeasmin, M.S. Islam, M. Rahman, S. Fendorf, N.M. Ardoin, P.J. Winch, S.P. Luby, Turmeric means "yellow" in Bengali: Lead chromate pigments added to turmeric threaten public health across Bangladesh, Environ. Res. 179 (2019) 108722. https://doi.org/10.1016/j.envres.2019.108722.

[10] R. Levin, C.L. Zilli Vieira, M.H. Rosenbaum, K. Bischoff, D.C. Mordarski, M.J. Brown, The urban lead (Pb) burden in humans, animals and the natural environment, Environ. Res. 193 (2021) 110377. https://doi.org/10.1016/j.envres.2020.110377.

[11] L.H. Nowell, P.W. Moran, R.J. Gilliom, D.L. Calhoun, C.G. Ingersoll, N.E. Kemble, K.M. Kuivila, P.J. Phillips, Contaminants in stream sediments from seven United States metropolitan areas: part I: distribution in relation to urbanization, Arch. Environ. Contam. Toxicol. 64 (2013) 32–51. https://doi.org/10.1007/s00244-012-9813-0.

[12] Directive 2008/105/EC of the European Parliament and of the Council of 16 December 2008 on environmental quality standards in the field of water policy, in: 2008.

[13] National Primary Drinking Water Regulations, , Title 40, Chapter 1, Subchapter D, Part 141, Subpart 1, Control of Lead and Copper, in: Code Fed. Regul., 2021.

[14] K. Haupt, K. Mosbach, Molecularly Imprinted Polymers and Their Use in Biomimetic Sensors, Chem. Rev. 100 (2000) 2495–2504. https://doi.org/10.1021/cr990099w.

[15] Y. El Ouardi, A. Giove, M. Laatikainen, C. Branger, K. Laatikainen, Benefit of ion imprinting technique in solid-phase extraction of heavy metals, special focus on the last decade, J. Environ. Chem. Eng. 9 (2021) 106548. https://doi.org/10.1016/j.jece.2021.106548.

[16] L. Uzun, A.P.F. Turner, Molecularly-imprinted polymer sensors: realising their potential, Biosens. Bioelectron. 76 (2016) 131–144. https://doi.org/10.1016/j.bios.2015.07.013.

[17] O.S. Ahmad, T.S. Bedwell, C. Esen, A. Garcia-Cruz, S.A. Piletsky, Molecularly Imprinted Polymers in Electrochemical and Optical Sensors, Trends Biotechnol. 37 (2019) 294–309. https://doi.org/10.1016/j.tibtech.2018.08.009.

[18] C. Unger, P.A. Lieberzeit, Molecularly imprinted thin film surfaces in sensing: Chances and challenges, React. Funct. Polym. 161 (2021) 104855. https://doi.org/10.1016/j.reactfunctpolym.2021.104855.

[19] A.M. Stortini, M.A. Baldo, G. Moro, F. Polo, L.M. Moretto, Bio- and Biomimetic Receptors for Electrochemical Sensing of Heavy Metal Ions, Sensors. 20 (2020) 6800. https://doi.org/10.3390/s20236800.
[20] M.K. Bojdi, M.H. Mashhadizadeh, M. Behbahani, A. Farahani, S.S.H. Davarani, A. Bagheri, Synthesis, characterization and application of novel lead imprinted polymer nanoparticles as a high selective electrochemical sensor for ultra-trace determination of lead ions in complex matrixes, Electrochimica Acta. 136 (2014) 59–65. https://doi.org/10.1016/j.electacta.2014.05.095.
[21] S. Di Masi, A. Garcia Cruz, F. Canfarotta, T. Cowen, P. Marote, C. Malitesta, S.A. Piletsky, Synthesis and Application of Ion-Imprinted Nanoparticles in Electrochemical Sensors for Copper (II) Determination, ChemNanoMat. 5 (2019) 754–760. https://doi.org/10.1002/cnma.201900056.
[22] M.K.L. Coelho, H.L.D. Oliveira, F.G.D. Almeida, K.B. Borges, C.R.T. Tarley, A.C. Pereira, Development of carbon paste electrode modified with cadmium ion-imprinted polymer for selective voltammetric determination of Cd2+, Int. J. Environ. Anal. Chem. 97 (2017) 1378–1392. https://doi.org/10.1080/03067319.2018.1424330.
[23] W. Wan, S. Wagner, K. Rurack, Fluorescent monomers: “bricks” that make a molecularly imprinted polymer “bright,” Anal. Bioanal. Chem. 408 (2016) 1753–1771. https://doi.org/10.1007/s00216-015-9174-4.
[24] Q. Yang, J. Li, X. Wang, H. Peng, H. Xiong, L. Chen, Strategies of molecular imprinting-based fluorescence sensors for chemical and biological analysis, Biosens. Bioelectron. 112 (2018) 54–71. https://doi.org/10.1016/j.bios.2018.04.028.
[25] H. Lu, C. Yu, S. Xu, A dual reference ion-imprinted ratiometric fluorescence probe for simultaneous detection of silver (I) and lead (II), Sens. Actuators B Chem. 288 (2019) 691–698. https://doi.org/10.1016/j.snb.2019.03.069.
[26] J. Qi, B. Li, X. Wang, Z. Zhang, Z. Wang, J. Han, L. Chen, Three-dimensional paper-based microfluidic chip device for multiplexed fluorescence detection of Cu2+ and Hg2+ ions based on ion imprinting technology, Sens. Actuators B Chem. 251 (2017) 224–233. https://doi.org/10.1016/j.snb.2017.05.052.
[27] T.H. Nguyen, T. Sun, K.T.V. Grattan, A Turn-On Fluorescence-Based Fibre Optic Sensor for the Detection of Mercury, Sensors. 19 (2019) 2142. https://doi.org/10.3390/s19092142.
[28] S. Lee, B.A. Rao, Y.-A. Son, A highly selective fluorescent chemosensor for Hg2+ based on a squaraine–bis(rhodamine-B) derivative: Part II, Sens. Actuators B Chem. 210 (2015) 519–532. https://doi.org/10.1016/j.snb.2015.01.008.
[29] S. Al-Kindy, R. Badía, M.E. Díaz-García, Fluorimetric Monitoring of Molecular Imprinted Polymer Recognition Events for Aluminium, Anal. Lett. 35 (2002) 1763–1774. https://doi.org/10.1081/AL-120013581.
[30] H. Sun, J.-P. Lai, D.-S. Lin, X.-X. Huang, Y. Zuo, Y.-L. Li, A novel fluorescent multi-functional monomer for preparation of silver ion-imprinted fluorescent on–off chemosensor, Sens. Actuators B Chem. 224 (2016) 485–491. https://doi.org/10.1016/j.snb.2015.10.052.
[31] J. Tan, H.-F. Wang, X.-P. Yan, A fluorescent sensor array based on ion imprinted mesoporous silica, Biosens. Bioelectron. 24 (2009) 3316–3321. https://doi.org/10.1016/j.bios.2009.04.024.
[32] W. René, M. Arab, K. Laatikainen, S. Mounier, C. Branger, V. Lenoble, Identifying the Stoichiometry of Metal/Ligand Complex by Coupling Spectroscopy and Modelling: a Comprehensive Study on Two Fluorescent Molecules Specific to Lead, J. Fluoresc. 29 (2019) 933–943. https://doi.org/10.1007/s10895-019-02405-0.
[33] W. René, V. Lenoble, M. Chioukh, C. Branger, A turn-on fluorescent ion-imprinted polymer for selective and reliable optosensing of lead in real water samples, Sens. Actuators B Chem. 319 (2020) 128252. https://doi.org/10.1016/j.snb.2020.128252.
[34] R.G. Zepp, W.M. Sheldon, M.A. Moran, Dissolved organic fluorophores in southeastern US coastal waters: correction method for eliminating Rayleigh and Raman scattering peaks in excitation–emission matrices, Mar. Chem. 89 (2004) 15–36. https://doi.org/10.1016/j.marchem.2004.02.006.
[35] M. Laatikainen, K. Laatikainen, S.-P. Reinikainen, H. Hyvönen, C. Branger, H. Siren, T. Sainio, Complexation of Nickel with 2-(Aminomethyl)pyridine at High Zinc Concentrations or in a Nonaqueous Solvent Mixture, J. Chem. Eng. Data. 59 (2014) 2207–2214. https://doi.org/10.1021/je500164h.

[36] P. Gans, A. Sabatini, A. Vacca, SUPERQUAD: an improved general program for computation of formation constants from potentiometric data, J. Chem. Soc. Dalton Trans. 0 (1985) 1195–1200. https://doi.org/10.1039/DT9850001195.
[37] K. Laatikainen, D. Udomsap, H. Siren, H. Brisset, T. Sainio, C. Branger, Effect of template ion–ligand complex stoichiometry on selectivity of ion-imprinted polymers, Talanta. 134 (2015) 538–545. https://doi.org/10.1016/j.talanta.2014.11.050.
[38] K. Laatikainen, C. Branger, B. Coulomb, V. Lenoble, T. Sainio, In situ complexation versus complex isolation in synthesis of ion imprinted polymers, React. Funct. Polym. 122 (2018) 1–8. https://doi.org/10.1016/j.reactfunctpolym.2017.10.022.
[39] A. Beltran, F. Borrull, R.M. Marcé, P.A.G. Cormack, Molecularly-imprinted polymers: useful sorbents for selective extractions, TrAC Trends Anal. Chem. 29 (2010) 1363–1375. https://doi.org/10.1016/j.trac.2010.07.020.
[40] W.-H. Li, H.D.H. Stöver, Monodisperse Cross-Linked Core−Shell Polymer Microspheres by Precipitation Polymerization, Macromolecules. 33 (2000) 4354–4360. https://doi.org/10.1021/ma9920691.
[41] T. Alizadeh, S. Amjadi, Preparation of nano-sized Pb2+ imprinted polymer and its application as the chemical interface of an electrochemical sensor for toxic lead determination in different real samples, J. Hazard. Mater. 190 (2011) 451–459. https://doi.org/10.1016/j.jhazmat.2011.03.067.
[42] V. Lenoble, W. Meouche, K. Laatikainen, C. Garnier, H. Brisset, A. Margaillan, C. Branger, Assessment and modelling of Ni(II) retention by an ion-imprinted polymer: Application in natural samples, J. Colloid Interface Sci. 448 (2015) 473–481. https://doi.org/10.1016/j.jcis.2015.02.055.
[43] J. Otero-Romaní, A. Moreda-Piñeiro, P. Bermejo-Barrera, A. Martin-Esteban, Synthesis, characterization and evaluation of ionic-imprinted polymers for solid-phase extraction of nickel from seawater, Anal. Chim. Acta. 630 (2008) 1–9. https://doi.org/10.1016/j.aca.2008.09.049.
[44] M.S. Jagirani, A. Balouch, S.A. Mahesar, A. Kumar, A.R. Baloch, Abdullah., M.I. Bhanger, Fabrication of cadmium tagged novel ion imprinted polymer for detoxification of the toxic Cd2+ion from aqueous environment, Microchem. J. 158 (2020) 105247. https://doi.org/10.1016/j.microc.2020.105247.
[45] K.S.W. Sing, Reporting physisorption data for gas/solid systems with special reference to the determination of surface area and porosity (Recommendations 1984), Pure Appl. Chem. 57 (1985) 603–619. https://doi.org/10.1351/pac198557040603.
[46] G. Limousin, J.-P. Gaudet, L. Charlet, S. Szenknect, V. Barthès, M. Krimissa, Sorption isotherms: A review on physical bases, modeling and measurement, Appl. Geochem. 22 (2007) 249–275. https://doi.org/10.1016/j.apgeochem.2006.09.010.
[47] E. Corton, J.A. García-Calzón, M.E. Díaz-García, Kinetics and binding properties of cloramphenicol imprinted polymers, J. Non-Cryst. Solids. 353 (2007) 974–980. https://doi.org/10.1016/j.jnoncrysol.2006.12.066.
[48] G.L. Long, J.D. Winefordner, Limit of detection. A closer look at the IUPAC definition, Anal. Chem. 55 (1983) 712A-724A.
[49] V. Thomsen, D. Schatzlein, D. Mercuro, Limits of detection in spectroscopy, Spectroscopy. 18 (2003) 112–114.
[50] Guidelines for drinking-water quality, in: WHO Library Cataloguing-in-Publication Data, 4th Edition, 2011.